Inhibition of primary ciliogenesis enhances efficacy of EGFR-TKIs against non-small cell lung cancer cells

LIANGLIANG JIN[1*], LI WEI[2*], JUNRUI HUA[3*], RONG ZHANG[4], JIAXIN CHEN[4], JINPENG HE[3] and YANLI YANG[1]

[1]Department of Pathology, The 940th Hospital of Joint Logistics Support Force of Chinese People's Liberation Army, Lanzhou, Gansu 730050, P.R. China; [2]NHC Key Laboratory of Diagnosis and Therapy of Gastrointestinal Tumor & Clinical Lab, Gansu Provincial Hospital, Lanzhou, Gansu 730000, P.R. China; [3]Key Laboratory of Space Radiobiology of Gansu, Institute of Modern Physics, Chinese Academy of Sciences, Lanzhou, Gansu 73000, P.R. China; [4]School of Basic Medical Sciences & School of Public Health, Gansu University of Chinese Medicine, Lanzhou, Gansu 730000, P.R. China

Received June 23, 2025; Accepted September 18, 2025

DOI: 10.3892/or.2025.9035

Abstract. Primary cilia are antenna-like organelles on almost all human cells that sense and transduce extracellular cues into cellular response. Primary cilia have been reported to be implicated in drug resistance in several cancer types, but their roles in cellular response to epidermal growth factor receptor (EGFR)-tyrosine kinase inhibitors (TKIs) in non-small cell lung cancer (NSCLC) are still not fully understood. In the present study, it was reported that primary cilia are more prevalent in EGFR-TKI-insensitive A549 and H23 cells compared with the drug-sensitive HCC827 and PC9 cells by immunofluorescence staining assay. Importantly, treatment with EGFR-TKIs (gefitinib and dacomitinib) results in a dose-dependent increase in cilia number and length in A549 and H23 cells, an effect not observed in HCC827 and PC9 cells. Upon administration of gefitinib, A549 cells predominantly arrest in the G1 phase detected by flow cytometric analysis, with a minority undergoing cell death and the majority entering senescence. Inhibition of ciliogenesis through the knockdown of IFT88 or ARL13B by targeted small interfering RNAs markedly enhances the sensitivity of A549 cells to EGFR-TKIs by promoting a shift from senescence to cell death. Furthermore, it was demonstrated by immunoblotting and immunofluorescence colocalization analysis that both the expression and ciliary localization of adenylate cyclase 3 (AC3) are significantly upregulated following EGFR-TKIs treatment, and the reduction of AC3 expression effectively mitigates cellular drug resistance in A549 cells. These findings highlight a critical role for the cilia-AC3 axis in modulating cellular response to EGFR-TKIs, suggesting it as a potential therapeutic target for the treatment of NSCLC.

Correspondence to: Dr Jinpeng He, Key Laboratory of Space Radiobiology of Gansu, Institute of Modern Physics, Chinese Academy of Sciences, 509 Nanchang Road, Lanzhou, Gansu 73000, P.R. China
E-mail: hejp03@impcas.ac.cn

Dr Yanli Yang, Department of Pathology, The 940th Hospital of Joint Logistics Support Force of Chinese People's Liberation Army, 333 South Binhe Road, Lanzhou, Gansu 730050, P.R. China
E-mail: a06974723@163.com

*Contributed equally

Key words: non-small cell lung cancer, epidermal growth factor receptor-tyrosine kinase inhibitors, primary cilia, adenylate cyclase 3

Introduction

Lung cancer (LC) remains the leading cancer type in morbidity and mortality worldwide (1), with non-small cell LC (NSCLC) representing the most prevalent subtype, accounting for ~85% of all LC cases (2). The aberrant activation of the epidermal growth factor receptor (EGFR) signaling pathway is a key driver of NSCLC (2). EGFR-tyrosine kinase inhibitors (TKIs) targeted therapy has demonstrated significant benefits in patients with NSCLC harboring activating EGFR mutation (3). Moreover, although the response rate to EGFR-TKIs is substantially lower in patients with NSCLC with wild-type EGFR compared with those with mutated EGFR (4), clinical trials indicate that EGFR-TKIs, when used as consolidation and maintenance treatment following first-line chemotherapy, can improve outcomes in patients with NSCLC with wild-type EGFR (5). Nevertheless, the efficacy of EGFR-TKIs is considerably constrained by intrinsic and acquired resistance, and the underlying mechanisms of EGFR-TKIs resistance are complicated and heterogeneous, encompassing secondary mutation in the target kinase domain, activation of alternative signal pathways, concurrent alteration in other oncogenes, histological transformation, and tumor microenvironment (6), which remains incompletely understood.

Primary cilia are ubiquitous, hair-like organelles that projected from cell surface, originating from the basal body and composed of an axoneme with a 9+0 microtubule doublet

configuration (7). The organelle functions as distinctive sensory structure and signaling hub, sensing and transducing extracellular chemical and physical stimuli into intracellular responses by coordinating multiple signaling pathways, including Hedgehog (HH), G protein-coupled receptor, receptor tyrosine kinase (RTK), and WNT pathways (8). Alterations in ciliation and ciliary signaling pathway status are significantly associated with various cancer types, but the role of cilia varies depending on the cancer type, stage and microenvironment (9). Notably, primary cilia have been implicated in resistance to chemotherapeutic agents (10-12), ionizing radiation (12,13), and protein kinase targeted inhibitors (14,15), suggesting a regulatory role in cellular response and resistance to cancer therapies.

It has been previously reported that the EGFR-TKI gefitinib (Gef) remarkably restores ciliogenesis in NSCLC A549 cells, as well as in kidney cancer UMRC2, breast cancer SUM159, and pancreatic cancer L3.6 cells (16). Furthermore, a notable increase in cilia frequency, length and fragmentation has been observed in NSCLC HCC4006, H2228, A549 and H23 cells that have developed resistance to kinase inhibitors, and ablation of cilia or inhibition of the cilia-dependent HH signaling pathway is sufficient to overcome both acquired and *de novo* kinase inhibitor resistance in NSCLC cells (14). These findings highlight the involvement of primary cilia in promoting EGFR-TKIs resistance in NSCLC, but the precise role and underlying mechanism are still largely unexplored.

The adenylate cyclase (AC) superfamily, which comprises nine membrane-bound subtypes (AC1-AC9) and one soluble subtype, plays critical roles in development, progression and therapy resistance across various cancer types by modulating the cyclic adenosine monophosphate (cAMP) signaling pathway (17). This pathway's activation and transduction are often orchestrated by primary cilia (18). AC3 is commonly localized to primary cilia in mammals and is involved in the regulation of cilia elongation and HH signaling (19,20). While emerging evidence has linked AC3 to cell proliferation, migration and invasion in gastric and pancreatic cancers (21,22), its role in EGFR-TKIs' resistance mechanisms in NSCLC remains to be fully elucidated.

In the present study, the prevalence of primary cilia in EGFR-TKIs' insensitive and sensitive NSCLC cells, as well as the dynamic alterations in ciliogenesis following EGFR-TKIs treatment were investigated. The functional roles of primary cilia and AC3 in modulating cellular responses to EGFR-TKIs were further studied, which may help to provide a novel strategy for overcoming drug resistance in NSCLC cells.

Materials and methods

Reagents. The first and second generation of EGFR-TKIs gefitinib (Gef; cat. no. HY-50895) and dacomitinib (Dac; cat. no. HY-13272) were purchased from MedChemExpress. Dimethyl sulfoxide (DMSO; cat. no. 472301) and propidium iodide (PI; 1.0 μg/ml; cat. no. P4864) were obtained from Sigma-Aldrich; Merck KGaA. For immunoblotting experiment, the primary antibodies of ERK (1:1,000; cat. no. ab184699) and phosphorylated-ERK (p-ERK; 1:1,000; cat. no. ab201015) were purchased from Abcam; primary antibodies of BCL2 (1:2,000; cat. no. 12789-1-AP), α-tubulin (α-tub; 1:40,000; cat. no. 11224-1-AP), IFT88 (1:1,000; cat. no. 60227-1-Ig), AC3 (1:1,000; cat. no. 19492-1-AP), Cyclin A2 (CCNA; 1:1,000; cat. no. 18202-1-AP), Cyclin B1 (CCNB; 1:1,000; cat. no. 55004-1-AP), Cyclin D1 (CCND; 1:3,000; cat. no. 60186-1-Ig), Cyclin E1 (CCNE; 1:1,000; cat. no. 11554-1-AP), CDK1 (1:1,000; cat. no. 19532-1-AP), CDK2 (1:1,000; cat. no. 10122-1-AP), p21 (1:1,000; cat. no. 10355-1-AP), p16 (1:1,000; cat. no. 10883-1-AP), GAPDH (1:50,000; cat. no. 60004-1-Ig), and the secondary antibodies including HRP-conjugated goat anti-mouse IgG (1:5,000; cat. no. SA00001-1), HRP-conjugated goat anti-rabbit IgG (1:5,000; cat. no. SA00001-2) were supplied by Proteintech Group, Inc. For immunofluorescence staining, the primary antibodies of ADP ribosylation factor such as GTPase 13B (ARL13B; 1:500; cat. no. 17711-1-AP/66739-1-Ig), AC3 (1:500; cat. no. 19492-1-AP) and γ-tubulin (γ-tub; 1:500; cat. no. T6557) were purchased from Proteintech Group, Inc. and Sigma-Aldrich; Merck KGaA respectively. The secondary antibodies including Alexa Fluor 594-conjugated goat anti-mouse IgG, Alexa Fluor 594-conjugated goat anti-mouse IgG (1:500; cat. no. A-11005), Alexa Fluor 488-conjugated goat anti-mouse IgG (1:500; cat. no. A-11001), Alexa Fluor Plus 555-conjugated goat anti-rabbit IgG (1:500; cat. no. A32732), and Alexa Fluor Plus 488-conjugated goat anti-rabbit IgG (1:500; cat. no. A32731) were purchased from Thermo Fisher Scientific, Inc. 4',6-diamidino-2-phenylindole (DAPI) was obtained from Molecular Probes; Thermo Fisher Scientific, Inc.

Cell culture. The human NSCLC cell lines A549 (CSTR: 19375.09.3101HUMSCSP503), NCI-H23 (H23; CSTR: 19375.09.3101HUMSCSP581), PC9 (CSTR: 19375.09.3101HUMSCSP5085) and HCC827 (CSTR: 19375.09.3101HUMSCSP538) were purchased from the Cell Bank/Stem Cell Bank, Chinese Academy of Sciences. A549 cells were cultured in Dulbecco's Modified Eagle Medium/F-12 (Gibco; Thermo Fisher Scientific, Inc.). H23, PC9 and HCC827 cells were maintained in RPMI-1640 medium (Gibco; Thermo Fisher Scientific, Inc.). The medium was supplemented with 10% fetal bovine serum (Shanghai ExCell Biology, Inc.), 100 units/ml penicillin and 100 μg/ml streptomycin (Beijing Solarbio Science & Technology Co., Ltd.). Cells were cultured in a humidified atmosphere at 37˚C under 5% CO_2, and tested negative for mycoplasma.

Cell viability assay. NSCLC cells ($1x10^5$) were planted in 6-well plates and incubated for 24 h, followed by treated with indicated concentrations of Gef or Dac for 48 h. In addition, NSCLC cells ($1x10^5$) were seeded in 6 well-plates for 24 h before transfected with siIFT88, siARL13B, siAC3, or NC. After transfection, Gef, Dac, or DMSO was immediately added into the medium and the cells were continuously cultured for 48 h. The cell number was counted using a Coulter counter (Z2; Beckman Coulter Inc.), the cell viability related to control group was determined and the half maximal inhibitory concentration (IC_{50}) of Gef or Dac was calculated.

Immunofluorescence staining. Cells were fixed with 4% paraformaldehyde (Beijing Solarbio Science & Technology Co., Ltd.) for 10 min at room temperature following the pre-chilling methanol at -20˚C for 20 min. The fixed cells

were permeabilized with 0.5% Triton X-100 for 10 min, then blocked with 5% immunostaining blocking buffer (Shanghai Yeasen Biotechnology Co., Ltd.) for 1 h at room temperature. The primary antibodies of ARL13B and γ-tub were used to visualize primary cilia and basal bodies, respectively. The primary antibody of AC3 was used to visualize its localization. The primary antibodies were incubated for 2 h at room temperature and then cells were incubated with the secondary antibodies for 1 h. The cell nuclei were counterstained with DAPI. The images were captured under an RVL-100-G fluorescence microscope (ECHO). For cilia frequency analysis, confidence level (α): 95%, Z-score: 1.96, margin of error (e): 5%, population proportion (p): 1-60%, when p=60% the population size (n)=369, and more than 500 cells for each experiment were calculated. For AC3 positive cilia analysis, confidence level (α): 95%, Z-score: 1.96, margin of error (e): 5%, population proportion (p): 0-20%, when p=20% the population size (n)=246, and more than 200 cilia were calculated for each group. The length of the primary cilium (n>50) was measured using ImageJ software (Version 1.52; National Institutes of Health).

Western blotting. Cells were lysed with RIPA buffer (Beyotime Institute of Biotechnology). The total cellular proteins (20 μg) were separated by 10% SDS-PAGE and transferred to a methanol-activated PVDF membrane (Merck KGaA). The membrane was blocked with 5% protein-free rapid blocking buffer (Wuhan Servicebio Technology Co., Ltd.) for 2 h at room temperature and probed with the primary antibodies for 2 h at room temperature. After incubation with HRP-conjugated secondary antibody, the protein bands were detected with chemiluminescence reagents (Merck KGaA), and the images were captured by using Alliance LD4 gel imaging system (UVITEC) and analyzed using ImageJ software.

Cell cycle distribution analysis. For the cell cycle assay, cells treated with Gef or Dac for 1-3 days were harvested and fixed in -20˚C pre-chilled 70% alcohol overnight, then stained with 20 μg/ml PI for 15 min at room temperature. Flow cytometric analysis was performed using Amnis imaging flow cytometer (Merck KGaA), and at least 10,000 gated events were acquired from each sample. The data were analyzed with Amnis IDEAS Application v6.0 (Merck KGaA).

PI staining. The control cells or cells transfected with small interfering RNAs (siRNAs) were treated with Gef or Dac for indicated time, then incubated with 20 μg/ml PI for 15 min to stain the dead cells. The images of bright field (BF) and fluorescence field were captured by using a DMI6000 fluorescence microscope (Leica Microsystems GmbH), and at least 500 cells were counted for each group.

RNA interference. Two individual stealth siRNAs targeting IFT88 (siIFT88-1/2, 25 nM, Thermo Fisher Scientific, Inc.) or ARL13B (siARL13B-1/2; 50 nM; Guangzhou RiboBio Co., Ltd.) were introduced into the cells by using Lipofectamine 2000 reagent (Thermo Fisher Scientific, Inc.) to ablate primary cilia. Three individual siRNAs against AC3 (Guangzhou RiboBio Co., Ltd.) were employed to knockdown the target gene expression at a final concentration of 50 nM. A negative control siRNA (NC; siN0000001-1-5; Guangzhou RiboBio Co., Ltd.) was used as the control group. Cells were transfected with siRNAs for 5 h at 37˚C and then the medium was replaced with fresh culture medium. The interference efficiency of siRNAs was evaluated by immunoblotting analysis. The sequences of siRNAs are as follows: siIFT88-1: 5'-CCAAAG CCAUUAAAUUCUACCGAAU-3'; siIFT88-2: 5'-GAAGAA AGCUGUAUUGCCAAUAGUU-3'; siARL13B-1: 5'-GTG TCAGATAGAACCATGT-3'; siARL13B-2: 5'-GAACCATGT TCAGCAATCT-3'; siAC3-1: 5'-GCACCAGCTTCCTCA AAGT-3'; siAC3-2: 5'-GGACTGGTGTTGGACATCA-3'; siAC3-3: 5'-GACGTATGATGAGATTGGA-3'. The sequences of NC were not provided for the commercial patent security protection.

Cell senescence assay. The cellular senescence was measured by Senescence-Tracker (Sen-Tra) assay as previously reported (23). Briefly, cells were exposed to DMSO or Gef (25 μM) for 1-3 days, followed by incubation with Sen-Tra fluorescence probe (10 μM; cat. no. C0603; Beyotime Institute of Biotechnology) overnight at 37˚C; then, the cells were washed with PBS for three times before imaging. The fluorescence images of senescent cells were captured on a DMI6000 fluorescence microscope. Quantification of images obtained from cells was performed using ImageJ software, and >500 cells were counted for each group.

Statistical analysis. All the experiments were repeated at least three times, and the data are presented as the mean ± standard deviation (SD). Statistical analysis was performed with Origin 2019 (OriginLab Corporation) using paired Student's t-test for two groups and one-way ANOVA followed by Tukey's post hoc test for multiple comparisons. $^{*}P<0.05$ was considered to indicate a statistically significant difference.

Results

EGFR-TKIs' insensitive and sensitive NSCLC cells present different ciliation status. To determine whether primary cilia are associated with cellular resistance to EGFR-TKIs in NSCLC, the drug-insensitive A549 and H23 cells (EGFR wild-type) and the drug-sensitive HCC827 and PC9 cells (EGFR mutant) were treated with increasing concentrations of Gef and Dac for 48 h to measure the IC_{50}. The results showed that the IC_{50} values for A549 and H23 to Gef/Dac are ~20.3/3.9 and 15.5/1.9 μM respectively (Fig. 1A and B; Fig. S1A and B), and that for HCC827/PC9 are significantly lower than 0.05/0.01 and 0.05/0.01 μM respectively (Fig. 1C and D; Fig. S1C and D). To further corroborate the distinct inhibitory effectiveness of EGFR-TKI on the drug-insensitive and drug-sensitive cells, the activation of ERK, a key EGFR downstream signaling factor (24), was detected in A549 and HCC827 cells challenged with different doses of Gef. As demonstrated, the expression level of activated ERK (p-ERK) exhibited a significant decrease in HCC827 but not in A549 cells (Fig. 1E and F), indicating that HCC827 is distinctly more sensitive to Gef and Dac than A549. Next, the immunofluorescence staining assay with the cilia and basal body markers ARL13B and γ-tub was performed, and typical primary cilia structure was observed in A549, H23 and HCC827 cells cultured in full

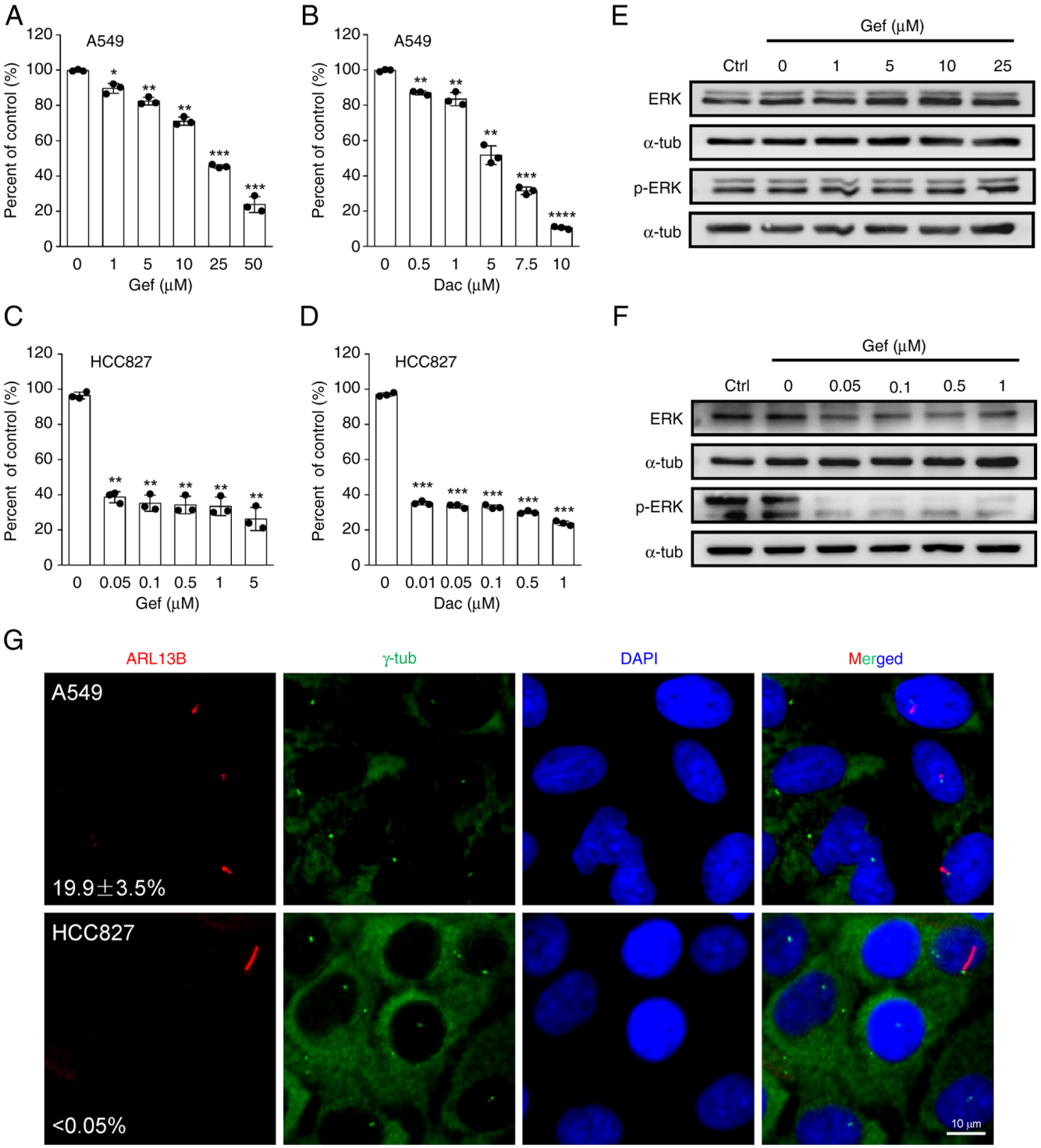

Figure 1. Epidermal growth factor receptor-tyrosine kinase inhibitor-insensitive A549 cells harbor high cilia incidence. (A and B) A549 cells were treated with increasing concentrations of (A) Gef or (B) Dac, and the cell viability related to untreated control (Ctrl) was measured at 48 h post-treatment. (C and D) HCC827 cells were treated with increasing concentrations of (C) Gef or (D) Dac, and the cell viability related to untreated control was measured at 48 h post-treatment. (E and F) A549 and HCC827 cells were exposed to increasing concentrations of Gef for 48 h, and the immunoblotting analysis was performed to measure the protein expression levels of ERK and p-ERK at Thr202/Tyr204. α-tubulin (α-tub) was used as a loading control. (G) Representative images of primary cilia labeled with ARL13B (red) and basal bodies labeled with γ-tub (green) in A549 and HCC827 cells, and the cilia incidence was calculated. The nuclei were counterstained with DAPI (blue). Scale bar, 10 μm. All quantitative data were obtained from three replicates and shown as the mean ± SD. Error bars, ± SD. *P<0.05, **P<0.01, ***P<0.001 and ****P<0.0001 compared with 0 μM (0.1% DMSO). Gef, gefitinib; Dac, dacomitinib; p-, phosphorylated; SD, standard deviation.

serum-containing medium (Figs. 1G and S2A), but that was completely lacking in PC9 cells (Fig. S2C). The cilia frequency is significantly higher in A549 (19.9±3.5%) and H23 (~1.5%) cells compared with that in HCC827 (<0.05%) and PC9 (none) cells (Figs. 1G and S2), suggesting a negative association between cilia incidence and cellular sensitivity to EGFR-TKIs.

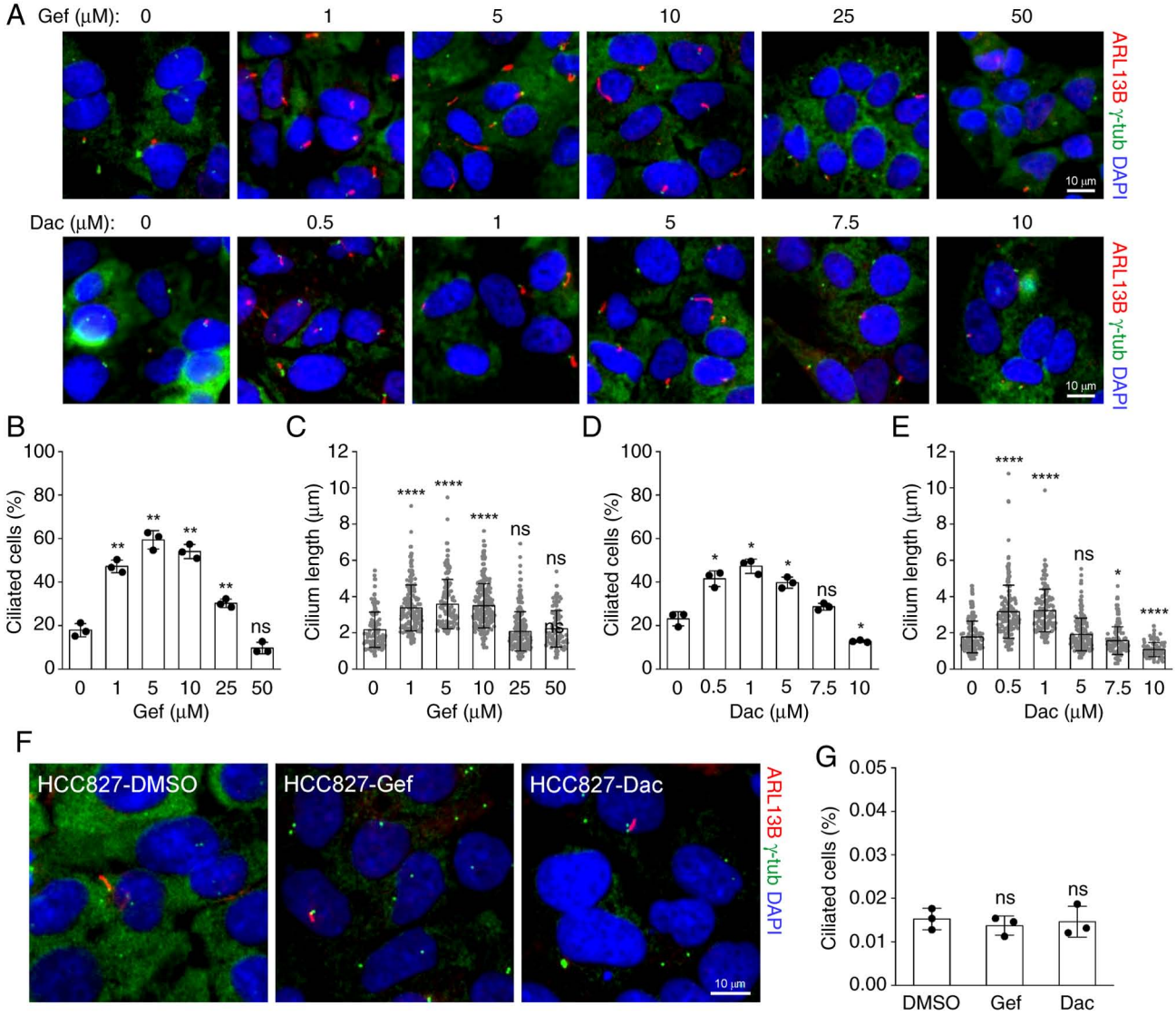

Figure 2. Epidermal growth factor receptor-tyrosine kinase inhibitors promote ciliogenesis in dose-dependent manner in A549 but not HCC827 cells. (A) Representative images of primary cilia labeled with ARL13B (red) and basal bodies labeled with γ-tub (green) in A549 cells treated with increasing doses of Gef or Dac for 48 h. (B and C) Quantification of (B) ciliated cells and the (C) cilium length of A549 cells treated with 0 (n=117), 1 (n=176), 5 (n=133), 10 (n=216), 25 (n=210), 50 (n=95) μM Gef for 48 h. **P<0.01 and ****P<0.0001 compared with 0 μM; ns, not significant. (D and E) Quantification of (D) ciliated cells and the (E) cilium length of A549 cells treated with 0 (n=133), 0.5 (n=153), 1 (n=138), 5 (n=163), 7.5 (n=130), 10 (n=80) μM Dac for 48 h. *P<0.05 and ****P<0.0001 compared with 0 μM; ns, not significant. (F) Representative images of primary cilia labeled with ARL13B (red) and basal bodies labeled with γ-tub (green) in HCC827 cells treated with 0.01 μM Gef or 0.001 μM Dac for 48 h. (G) Quantification of ciliated cells in HCC827 cells in (F). ns, not significant compared with DMSO. The nuclei were counterstained with DAPI (blue). Scale bar, 10 μm. All quantitative data were obtained from three replicates and shown as the mean ± SD. Error bars, ± SD. Gef, gefitinib; Dac, dacomitinib; p-, phosphorylated; SD, standard deviation; ns, not significant.

EGFR-TKIs facilitate primary cilia formation and elongation in A549 and H23 but not HCC827 and PC9 cells. Increased cilia frequency and length have been reported in TKI-resistant NSCLC cells, such as erlotinib-resistant HCC4006 (14) and dasatinib-resistant A549 cells (25), but no significant alterations in afatinib- and erlotinib-resistant PC9 cells compared with the parental cells (14). To investigate the effects of EGFR-TKIs on primary ciliogenesis in NSCLC cells, the A549, H23, HCC827 and PC9 cells were treated with multiple doses of Gef and Dac. As revealed in Fig. 2A-E, administration of Gef and Dac resulted in remarkable cilia formation and elongation in A549 cells in a dose-dependent manner. The proportion of ciliated cells was raised from ~20% in DMSO (0 μM Gef)-treated cells to nearly 60% in 5 μM Gef-treated cells, and to nearly 50% in 1 μM Dac-treated cells. Similar alterations were observed in H23 cells treated with 5 μM Gef or 1 μM Dac (Fig. S2A and B). As the drug concentration increased, the cilia incidence and length were gradually decreased, and exposure to 50 μM Gef or 10 μM Dac even lead to deciliation in A549 cells. However, Gef and Dac were not able to induce cilia formation in HCC827 and PC9 cells (Fig. 2F and G; Fig. S2C). Together, these data suggested that the ciliogenesis responding to EGF-TKIs maybe contribute to drug resistance in NSCLC cells.

EGFR-TKIs induce cytostatic but not cytotoxic effects. Next, the effects of EGF-TKIs on the cell cycle and cell fate were investigated. Upon Gef (25 μM) treatment, A549 cells were

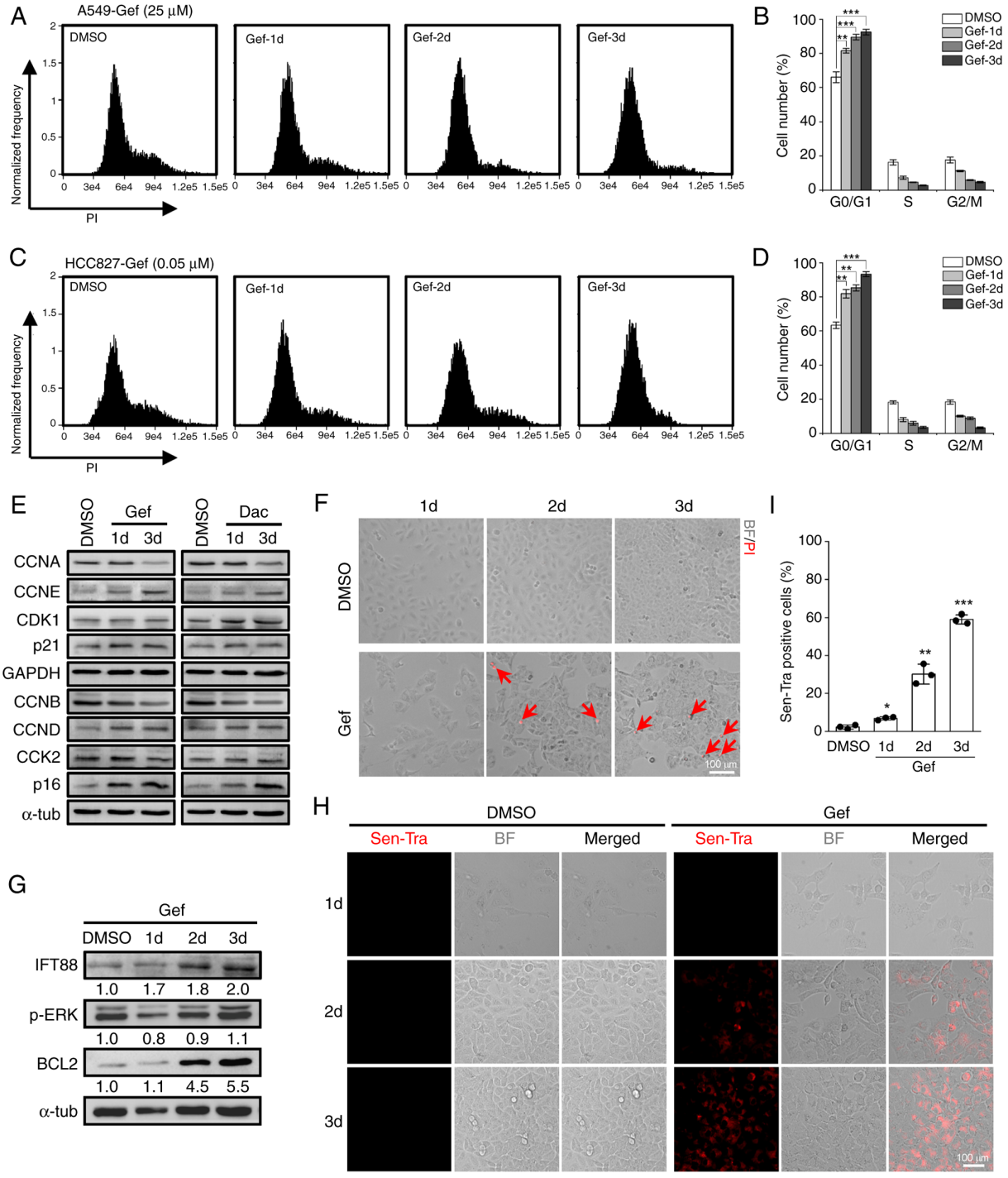

Figure 3. Gef treatment leads to G1 phase arrest and senescence. (A and B) Cell cycle distribution assay of A549 cells treated with DMSO (0.1%) or 25 μM Gef for 1, 2, and 3 days (d) by flow cytometry with (A) PI staining; (B) quantification data. (C and D) Cell cycle distribution assay of HCC827 cells treated with DMSO (0.1%) or 0.05 μM Gef for 1, 2, and 3 days by flow cytometry with (C) PI staining; (D) quantification data. (E) Immunoblotting analysis of the expression levels of CCNA, CCNB, CCND, CCNE, CDK1, CDK2, p16 and p21 in A549 cells treated with DMSO, Gef (25 μM), or Dac (5 μM) for 1 and 3 days. α-tubulin (α-tub) and GAPDH were used as loading controls. (F) Representative PI staining images of A549 cells exposed to DMSO (0.1%) or Gef (25 μM) for 1, 2, 3 days, the dead cells (red) were stained with PI and indicated with red arrows. Scale bar, 100 μm. (G) Immunoblotting analysis of the expression levels of IFT88, p-ERK (Thr202/Tyr204) and BCL2 in A549 cells treated with DMSO (0.1%) or Gef (25 μM) for 1, 2, 3 days. α-tubulin (α-tub) was used as a loading control. The values under the immunoblot bands indicate the quantitative densitometry value measured using ImageJ software. (H and I) The (H) cellular senescence assay of A549 cells treated with DMSO (0.1%) or Gef (25 μM) for 1-3 d labeling by senescence-tracker (Sen-Tra) fluorescence probe, and the (I) quantification data. Scale bar, 100 μm. Data are expressed as the mean ± SD. Error bars, ± SD. *P<0.05, **P<0.01 and ***P<0.001 compared with DMSO. Gef, gefitinib; PI, propidium iodide; CCNA, Cyclin A2; CCNB, Cyclin B1; CCND, Cyclin D1; CCNE, Cyclin E1; Dac, dacomitinib; BF, bright field; p-, phosphorylated; SD, standard deviation.

predominantly blocked in G0/G1 phase in a time-dependent manner (Fig. 3A and B). Similar phenomenon was observed in HCC827 exposed to 0.05 μM Gef (Fig. 3C and D). Moreover, the expression levels of G1 cyclins (CCND and CCNE) and cyclin-dependent kinase inhibitor (p16 and p21) were consistently upregulated following Gef and Dac treatment in A549

cells, while the expression levels of S and G2/M cyclins (CCNA and CCNB) were suppressed, and the cyclin-dependent kinase CDK1 and CDK2 showed slight changes (Fig. 3E), supporting a G1 phase arrest induced by EGFR-TKIs. Notably, Gef treatment resulted in little cell death in A549 cells; <5% dead cells were detected at 3 days post-treatment (Fig. 3F). The expression levels of p-ERK in Gef-treated cells showed modest reduction compared with the DMSO-treated group, but the positive ciliogenesis modulator IFT88 and the negative apoptosis regulator BCL2 were gradually elevated (Fig. 3G), indicating enhanced capacities of ciliogenesis and anti-apoptosis. Strikingly, increased senescent cells were detected by the Sen-Tra labeling assay in A549 cells exposed to 25 μM Gef (Fig. 3H), and the proportion of senescent cells reached ~60% at 3 days after Gef exposure (Fig. 3I). Collectively, these data demonstrated that EGFR-TKIs induce cytostatic but not cytotoxic effects in NSCLC cells.

Disruption of ciliogenesis attenuates cellular resistance to EGFR-TKIs. Given that Gef and Dac can promote primary cilia formation in A549 and H23 cells (Figs. 2A and S2A), it is likely that the primary cilia may play important roles in responding to EGFR-TKIs in the insensitive NSCLC cells. To determine this conjecture, the siRNAs targeting IFT88 (siIFT88-1/2) or ARL13B (siARL13B-1/2) were introduced into A549 cells. The results showed that transfection of siIFT88 or siARL13B prominently suppressed the protein expression levels of IFT88 or ARL13B in A549 cells (Fig. 4A). Moreover, knockdown of IFT88 or ARL13B by siRNAs resulted in significant decreases in the cilia frequency and length in A549 cells exposed to Gef as expected (Fig. 4B-D). Importantly, the ablation of primary cilia by siIFT88 and siARL13B profoundly improved the inhibitory efficacy of Gef and Dac against A549 cells (Fig. 4E and F). In addition, the PI staining assay revealed that the abrogation of ciliogenesis by IFT88 or ARL13b silencing strongly provoked the cell death in A549 cells exposed to 25 μM Gef (Fig. 4G), and the proportion of dead cells rose to ~30% at 3 days after treatment (Fig. 4H). These results indicated that the inhibition of ciliogenesis sensitizes A549 cells to EGFR-TKIs by switching senescence to cell death.

EGFR-TKIs promote AC3 expression and ciliary localization. To gain insight into the role for AC3 in primary cilia-mediated cellular resistance to EGFR-TKIs in NSCLC cells, the expression of AC3 in responding to Gef and Dac stresses in A549 cells were detected. As demonstrated in Fig. 5A, both Gef and Dac treatment leads to persistent upregulation of AC3 protein expression, which is in accordance with ciliary gene ARL13B protein expression. Previously, it has been reported that AC3 presents on primary cilia in multiple cell types such as synoviocyte (20) osteocyte (26) and astrocyte (27). To determine AC3 subcellular localization in NSCLC cells exposed to EGFR-TKIs, A549 cells were treated with DMSO (0.1%), Gef (10 μM) and Dac (5 μM) for 3 days followed by visualization of the primary cilia with immunofluorescence staining of antibodies against ARL13B, and the results identified that the proportion of AC3 positive cilia increased to >20% in Gef- and Dar-treated cells while that was merely found in DMSO-treated cells (Fig. 5B and C). However, EGFR-TKIs treatment slightly altered ARL13B expression levels and even decreased AC3 expression levels in HCC827 cells (Fig. 5D), indicating different responses of ciliogenesis and AC3 expression to EGFR-TKI stress between A549 and HCC827 cells. Furthermore, it was found that Gef-induced AC3 expression and ciliary localization were mitigated by disruption of primary cilia (Fig. 5E and F). Collectively, these results indicated that EGFR-TKI-induced AC3 expression and localization to primary cilia may contribute to cellular drug resistance.

Suppression of AC3 expression is sufficient to sensitize A549 cells to Gef. Given that EGFR-TKIs promote AC3 expression and presence on primary cilia, the role of AC3 in cellular EGFR-TKI sensitivity was investigated. Three individual siRNAs specifically against AC3 (siAC3-1/2/3) were introduced to suppress its protein expression (Fig. 6A), whereas the expression of ARL13b was merely affected upon siAC3 treatment. Subsequently, the cell viability was measured and the results showed that the cellular sensitivity was significantly enhanced in A549 cells transfected with siAC3 compared with that transfected with NC siRNA following Gef combination treatment at 0, 5 and 10 μM for 48 h (Fig. 6B), indicating a positive association between AC3, cell proliferation and drug resistance ability. Additionally, inhibition of AC3 could induce or reduce cilia elongation in different cell types (20,26), suggesting a feedback regulation of AC3 for ciliogenesis. To address this issue, the cilia frequency of A549 cells transfected with siAC3-1 or NC was detected following 10 μM Gef administrations for 48 h. However, it was found that the proportion of ciliated cells was barely altered upon AC3 suppression (Fig. 6C and D), indicating that EGFR-TKIs-induced cilia formation is not associated with AC3 expression and cilia localization.

Discussion

In the present study, it was demonstrated that EGFR-TKIs facilitate primary ciliogenesis in the drug-insensitive A549 and H23 cells but not in the drug-sensitive HCC827 and PC9 cells. Specifically, it was revealed that the disruption of primary cilia reduces cellular resistance to EGFR-TKIs, potentially linked to AC3 expression and its ciliary localization. Together, these results suggested a connection between the primary cilia-AC3 axis and cellular sensitivity to EGFR-TKIs in NSCLC.

Primary cilia, functioning as antennae on cell surface, play a crucial role in responding to extracellular signals by coordinate various signaling pathways that regulate cell proliferation, division, migration, metabolism and physiology (28). Despite the frequent loss or repression of primary cilia in numerous solid tumor types (9), an increasing number of small molecular anticancer drugs, including diverse protein kinase inhibitors, have been identified that can restore ciliogenesis in cancer cells (14,16,29,30). This restoration suppresses cancer progression and alters drug sensitivity simultaneously (31). In the EGFR-mutant NSCLS cell line HCC4006, which completely lacks primary cilia, sustained administration of the EGFR-TKI erlotinib results in acquired drug resistance and increased ciliogenesis (14). In the present study, the results revealed that EGFR-TKI *de novo*-resistant NSCLC A549 cells maintain a significantly larger population

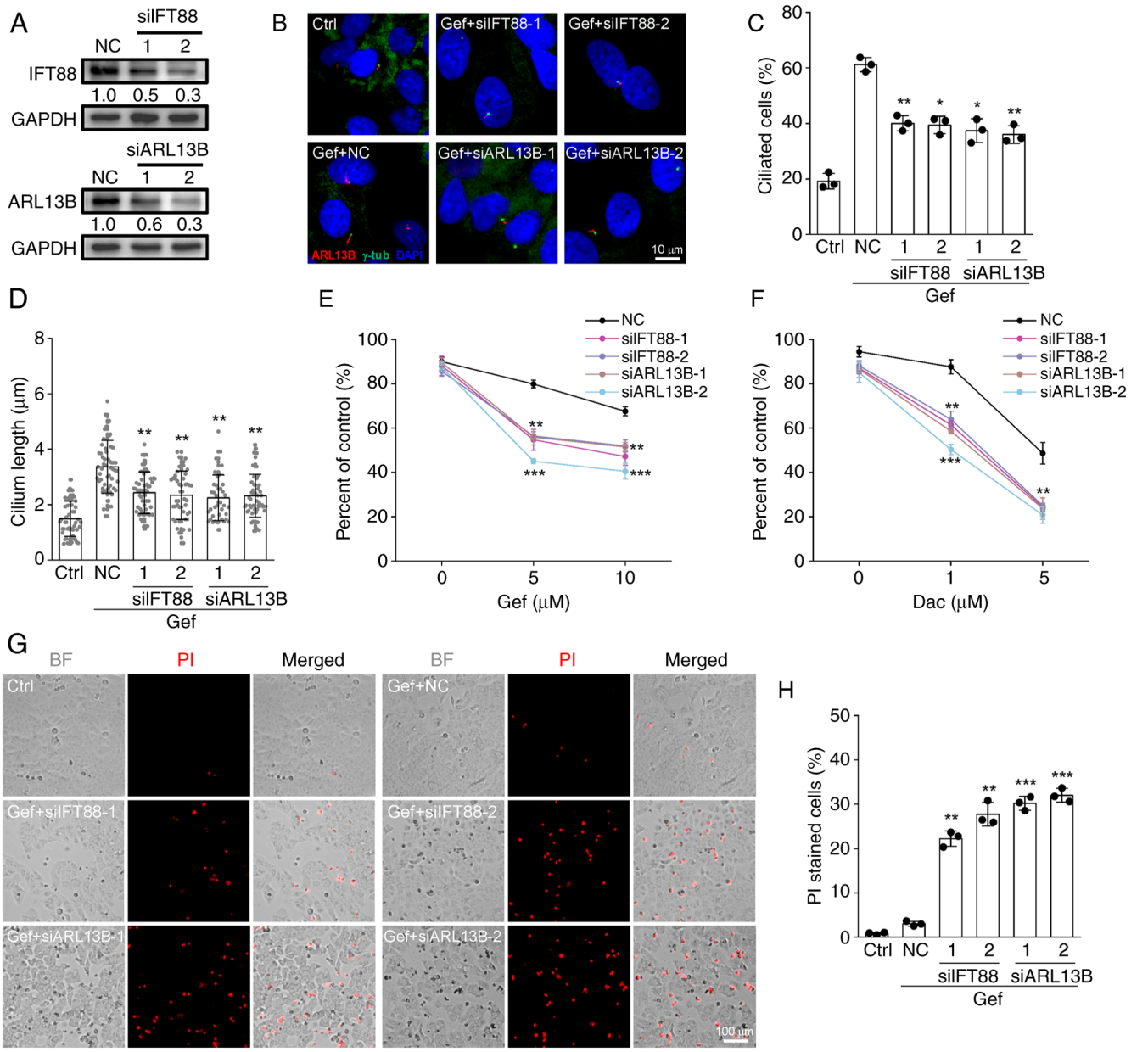

Figure 4. Inhibition of ciliogenesis sensitizes A549 cells to epidermal growth factor receptor-tyrosine kinase inhibitors. (A) Immunoblotting analysis of the protein expression levels of IFT88 and ARL13B in A549 cells transfected with siRNAs against IFT88 (siIFT88-1/2), ARL13B (siARL13B-1/2), or NC. GAPDH was employed as a loading control. The values under the immunoblot bands indicate the quantitative densitometry value measured using ImageJ software. (B-D) Immunofluorescence labeling of primary cilia (ARL13B, red) and basal bodies (γ-tub, green) in A549 control cells (Ctrl) and cells transfected with siIFT88-1/2, siARL13B-1/2, or NC following treated with 10 μM Gef for 48 h, (C) the proportion of ciliated cells and (D) cilium length in each group. Ctrl, n=52; Gef-NC, n=59; Gef-siIFT88-1, n=57; Gef-siIFT88-2, n=64; Gef-siARL13B-1, n=56; Gef-siARL13B-2, n=69. The nuclei were stained with DAPI (blue). (E and F) A549 cells transfected with NC, siIFT88-1/2, or ARL13B-1/2 siRNAs were exposed to (E) Gef (0, 5, 10 μM) or (F) Dac (0, 1, 5 μM) for 48 h, the cell viability related to untreated control was measured. (G and H) A549 cells transfected with indicated siRNAs were exposed 10 μM Gef for 48 h and stained with PI to detect the dead cells and quantification data for each group. Scale bar, 100 μm. Data are expressed as the mean ± SD. Error bars, ± SD. *P<0.05, **P<0.01 and ***P<0.001 compared with NC. siRNA, small interfering RNA; NC, negative control; Gef, gefitinib; Dac, dacomitinib; BF, bright field; SD, standard deviation.

of ciliated cells than drug-sensitive HCC827 cells (Fig. 1), and short-term exposure to Gef and Dac further enhances primary cilia formation in A549 and H23 cells but not in HCC827 and PC9 cells (Figs. 2 and S2), suggesting that primary cilia may be one of the EGFR-TKI resistance mechanisms in EGFR wild-type NSCLC compared with EGFR mutant type. Thus, these results robustly confirm the involvement of primary cilia in both the innate and adaptive resistance of NSCLC to EGFR-TKIs.

The molecular mechanisms underlying acquired resistance to EGFR-TKIs in NSCLC predominantly involve reactivation, bypass and indifference of the EGFR pathway (6). However, it remains limited in cancer types lacking mutations of the drug target, hindering the development and application of novel therapeutic strategies. As a distinctive sensory organelle, primary cilia play crucial role in cell fate determination in responding to anticancer drugs by regulating receptors located on cilia (32). Notably, EGFR has been shown to localize to

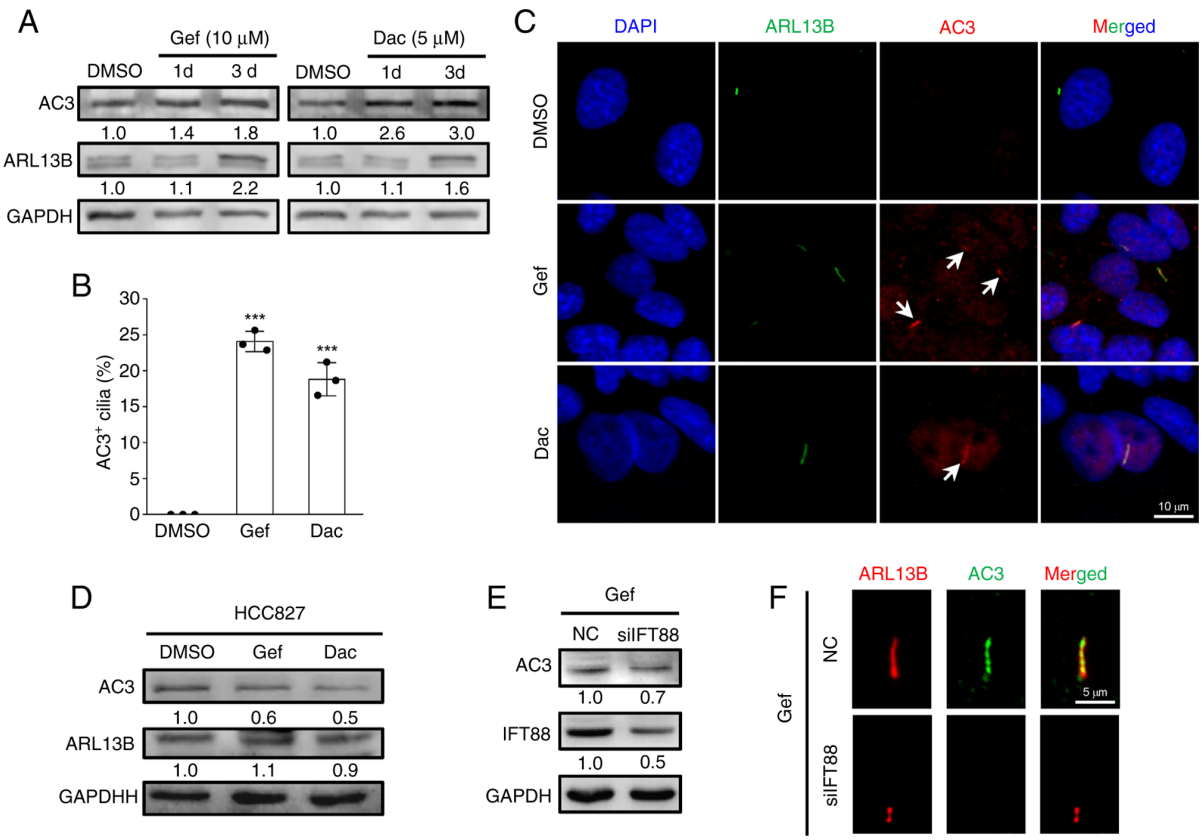

Figure 5. Epidermal growth factor receptor-tyrosine kinase inhibitors induce AC3 expression and ciliary localization. (A) Immunoblotting analysis of the expression levels of AC3 and ARL13B in A549 cells exposed to DMSO (0.1%), Gef (10 μM) and Dac (5 μM) for 1 and 3 days. (B and C) Immunofluorescence labeling of primary cilia (Arl13b, green) and AC3 (red, indicated by white arrows) in A549 cells administrated with DMSO (0.1%), Gef (10 μM), and Dac (5 μM) for 3 days, and quantification of AC3 positive (AC3$^+$) cilia in each group. The nuclei were stained with DAPI (blue). Scale bar, 10 μm. Data are expressed as the mean ± SD. Error bars, ± SD. ***P<0.001 compared with DMSO. (D) Immunoblotting analysis of the expression levels of AC3 and ARL13B in HCC827 cells exposed to DMSO (0.1%), Gef (0.05 μM) and Dac (0.01 μM) for 3 days. (E) Immunoblotting analysis of the protein expression levels of AC3 and IFT88 in Gef-treated A549 cells transfected with siIFT88-1 (siIFT88) or NC siRNA for 3 days. (F) Immunofluorescence labeling of primary cilia (Arl13b, red) and AC3 (green) in cells in (E). Scale bar, 5 μm. GAPDH was used as a loading control; the values under the immunoblot bands indicate the quantitative densitometry value measured using ImageJ software. Gef, gefitinib; Dac, dacomitinib; SD, standard deviation; si-, small interfering; NC, negative control; AC3, adenylate cyclase 3.

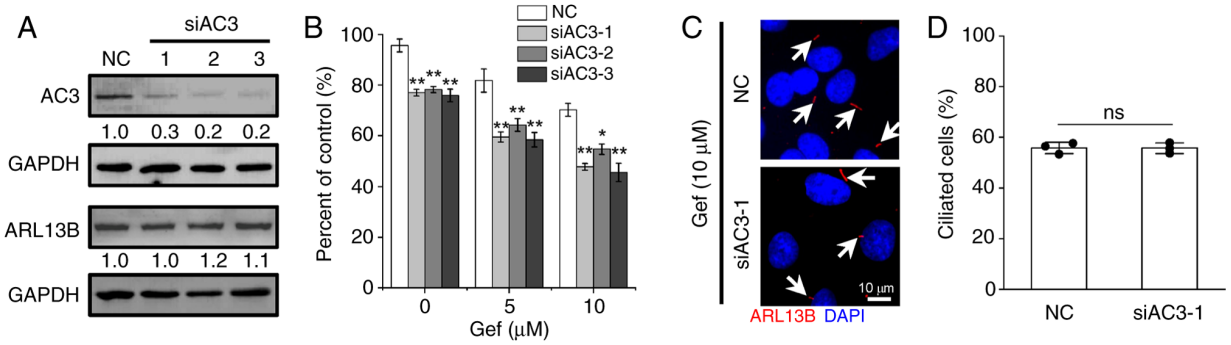

Figure 6. Silencing AC3 expression enhances cellular sensitivity to Gef. (A) Immunoblotting analysis of the expression levels of AC3 and ARL13B in A549 cells transfected with siRNAs targeting AC3 (siAC3-1/2/3) or NC for 48 h. GAPDH was used as a loading control. The values under the immunoblot bands indicate the quantitative densitometry value measured using ImageJ software. (B) A549 cells transfected NC or siAC3-1/2/3 were exposed to Gef (0, 5, 10 μM) for 48 h, the cell viability related to untreated control was measured. (C and D) Immunofluorescence labeling of primary cilia (Arl13b, red, indicated by white arrows) in A549 cells transfected with NC and siAC3-1 following administrated with Gef (10 μM) for 3 days, and quantification of ciliated cells in each group. The nuclei were stained with DAPI (blue). Scale bar, 10 μm. Data are expressed as the mean ± SD. Error bars, ± SD. *P<0.05 and **P<0.01 compared with NC. AC3, adenylate cyclase 3; Gef, gefitinib; si-, small interfering; NC, negative control; SD, standard deviation; ns, not significant.

primary cilia (33), where its signaling activity is restrict appropriately (33). Additionally, the aberrant activation of EGFR signaling leads to the loss of primary cilia via Aurora A in oral mucosa carcinoma and human retinal epithelia RPE1 cells (34,35), suggesting a negative feedback loop between primary cilia and EGFR.

Activation of the EGFR pathway drives cell proliferation, migration and metabolism through downstream effectors including the PI3K-AKT, JAK-STAT and RAS-RAF-MEK-ERK pathways (6). A recent study has uncovered the role of primary cilia in facilitating AKT and ERK activation induced by type A platelet-derived growth factor during Leydig cell development (36). Additionally, treatment with EGFR-TKIs significantly reduces proliferation without causing cell death in various cancer cells, with a process linked to YAP-mediated ciliogenesis (37,38). The present findings also demonstrated that A549 cells experienced strong G1 cell cycle arrest (Fig. 3A), formed cilia (Fig. 2A), and subsequently entered senescence (Fig. 3H) rather than undergoing cell death (Fig. 3F) after Gef and Dac treatment, implicating a positive relationship between primary cilia and senescence induced by EGFR-TKIs in NSCLC.

Accumulating evidence has highlighted the functional role of primary cilia in cell fate determination. Loss of primary cilia in thyroid cancer cells leads to apoptogenic stimuli and subsequent apoptotic cell death both *in vitro* and *in vivo* (39). Genotoxic stress-induced ciliogenesis drives cell senescence initiation and maintenance (13,40,41), the removal of cilia increases cellular sensitivity to ionizing radiation by inducing apoptosis in senescent cells (13). In the present study, results also revealed that the suppression of primary cilia by knockdown of ciliary gene IFT88 or ARL13B significantly enhanced the efficacy of EGFR-TKIs against NSCLC (Fig. 4E and F), potentially due to increased cell death (Fig. 4G and H). However, the specific type of cell death remains unconfirmed in the present study. Further investigation into the role of primary cilia in cell fate determination and the underlying mechanisms may facilitate the identification of novel therapeutic avenue to sensitize NSCLC to EGFR-TKIs.

Accumulating evidence indicates a reciprocal relationship between primary cilia and cellular senescence. Increased ciliogenesis have been observed in senescent cells triggered by various stimuli (13,42,43). Conversely, it has been demonstrated that primary ciliogenesis is an essential cellular process in senescence induction induced by etoposide (43) or ionizing radiation (13), mediated through autophagy or HH signaling activation in tumor cells. Furthermore, Ma *et al* (41) demonstrated that stress-induced transient primary ciliogenesis is required for senescence initiation in human fetal lung fibroblast IMR-90 cells exposed to ionizing radiation, oxidative stress, or inflammatory stimuli, and that these cilia disassemble after senescence entry (41). However, a recent study by the authors revealed persistent primary ciliogenesis in senescent tumor cells following ionizing radiation, which critically contributes to both the initiation and maintenance of senescence, and targeting either primary cilia or the senescence-associated BCL2 pathway with ABT-263 significantly enhanced the lethal effects of radiation (44). Therefore, targeting the crosstalk between primary cilia and senescence may represent an effective strategy for improving treatment efficacy.

The AC family numbers play a pivotal role in physiological and biological processes by modulating cAMP-related signaling pathways, primarily involving protein kinase A (PKA) and cAMP-activated guanine exchange factor (EPAC) (17,45). The upregulation of cAMP by AC1 has been shown to reduce apoptosis induced by DNA damage by promoting DNA damage repair mechanisms, thereby increasing cellular resistance to chemotherapy and radiotherapy (46,47). AC3, recognized as a marker for cilia, is localized within primary cilia in a cell type-dependent manner (19). In the present study, it was reported for the first time to the best of our knowledge, that EGFR-TKIs provoke the expression and ciliary localization of AC3 in NSCLC cells with wild-type EGFR that are insensitive to the drugs (Fig. 5A-C). Furthermore, the inhibition of AC3 expression was found to enhance the cytotoxic effects of EGFR-TKIs (Fig. 6). Although the downstream signaling pathways of AC3 were not investigated, it is imperative to focus on cAMP-PKA/EPAC pathways, as they are closely associated with senescence and survival (45). Understanding these factors is crucial for elucidating the mechanism of EGFR-TKI resistance mediated by the cilia-AC3 axis.

Although the present results suggest a potential functional interplay between primary cilia and cellular resistance to EGFR-TKIs in wild-type EGFR NSCLC, several limitations and open questions remain: i) While the present study discloses a novel association between primary cilia and intrinsic resistance to EGFR-TKIs, the absence of drug-resistant EGFR-mutant NSCLC cell models precludes conclusions about their role in acquired resistance; ii) neither alternative RTK pathway activation nor aberrant EGFR downstream pathway activation, two crucial resistance mechanisms (24), were examined, as well as their relationship to primary cilia; iii) increased cell death was observed in cilia-disrupted A549 cells treated with Gef using PI staining, a method that cannot distinguish type of cell death; iv) the study lacks *in vivo* validation using tumor-bearing animal models or patient-derived organoids to substantiate the functional role of primary cilia; and v) it was found that EGFR-TKI treatment promotes cilia formation (Fig. 2A-E) and AC3 ciliary localization (Fig. 5B and C), and the disruption of ciliogenesis and interference of AC3 expression increases cell sensitivity to EGFR-TKIs in A549 cells, whereas the involvement of AC3 downstream signaling, particularly the cAMP-PKA/EPAC pathway (45), in response to EGFR-TKI and its contribution to drug resistance remain unexplored. Further research is therefore required to elucidate the mechanisms by which the primary cilia-AC3 axis modulates EGFR-TKI resistance in NSCLC.

In conclusion, the present study revealed that the primary cilia-AC3 axis contributes to cellular resistance to EGFR-TKIs in NSCLC and underscores its potential as a sensitizing strategy for combination therapy in NSCLC.

Acknowledgements

The authors would like to thank Dr Dan Xu and Dr Qingfeng Wu (Biomedical Platform of the Public Technology Center, Institute of Modern Physics, Chinese Academy of Sciences) for providing technical assistance in flow cytometric analysis.

Funding

The present study was supported by the Non-profit Central Research Institute Fund of Chinese Academy of Medical Sciences (grant no. 2019PT320005), the Science and Technology Research Project of Gansu (grant nos. 23JRRA533,

24JRRA952 and 25JRRA1204), the National Natural Science Foundation of China (grant no. 12375355) and the Youth Innovation Promotion Association CAS (grant no. 2021415).

Availability of data and materials

The data generated in the present study may be requested from the corresponding author.

Authors' contributions

LJ, LW and JHu conducted investigation, curated data, developed methodology, acquired funding and wrote the original draft. RZ and JC conducted investigation and developed methodology. JHe and YY conceptualized and supervised the study, wrote, reviewed and edited the manuscript, and acquired funding. All authors read and approved the final version of the manuscript. JHe and YY confirm the authenticity of all the raw data.

Ethics approval and consent to participate

Not applicable.

Patient consent for publication

Not applicable.

Competing interests

The authors declare that they have no competing interests.

References

1. Bray F, Laversanne M, Sung H, Ferlay J, Siegel RL, Soerjomataram I and Jemal A: Global cancer statistics 2022: GLOBOCAN estimates of incidence and mortality worldwide for 36 cancers in 185 countries. CA Cancer J Clin 74: 229-263, 2024.
2. Hendriks LEL, Remon J, Faivre-Finn C, Garassino MC, Heymach JV, Kerr KM, Tan DSW, Veronesi G and Reck M: Non-small-cell lung cancer. Nat Rev Dis Primers 10: 71, 2024.
3. Pao W and Chmielecki J: Rational, biologically based treatment of EGFR-mutant non-small-cell lung cancer. Nat Rev Cancer 10: 760-774, 2010.
4. Inoue A, Suzuki T, Fukuhara T, Maemondo M, Kimura Y, Morikawa N, Watanabe H, Saijo Y and Nukiwa T: Prospective phase II study of gefitinib for chemotherapy-naive patients with advanced non-small-cell lung cancer with epidermal growth factor receptor gene mutations. J Clin Oncol 24: 3340-3346, 2006.
5. Cappuzzo F, Ciuleanu T, Stelmakh L, Cicenas S, Szczésna A, Juhász E, Esteban E, Molinier O, Brugger W, Melezínek I, *et al*: Erlotinib as maintenance treatment in advanced non-small-cell lung cancer: A multicentre, randomised, placebo-controlled phase 3 study. Lancet Oncol 11: 521-529, 2010.
6. Du Z, Kan H, Sun J, Liu Y, Gu J, Akemujiang S, Zou Y, Jiang L, Wang Q, Li C, *et al*: Molecular mechanisms of acquired resistance to EGFR tyrosine kinase inhibitors in non-small cell lung cancer. Drug Resist Updat 82: 101266, 2025.
7. Satir P, Pedersen LB and Christensen ST: The primary cilium at a glance. J Cell Sci 123: 499-503, 2010.
8. Anvarian Z, Mykytyn K, Mukhopadhyay S, Pedersen LB and Christensen ST: Cellular signalling by primary cilia in development, organ function and disease. Nat Rev Nephrol 15: 199-219, 2019.
9. Kiseleva AA, Nikonova AS and Golemis EA: Patterns of ciliation and ciliary signaling in cancer. Rev Physiol Biochem Pharmacol 185: 87-105, 2023.
10. Shireman JM, Atashi F, Lee G, Ali ES, Saathoff MR, Park CH, Savchuk S, Baisiwala S, Miska J, Lesniak MS, *et al*: De novo purine biosynthesis is a major driver of chemoresistance in glioblastoma. Brain 144: 1230-1246, 2021.
11. Chao YY, Huang BM, Peng IC, Lee PR, Lai YS, Chiu WT, Lin YS, Lin SC, Chang JH, Chen PS, *et al*: ATM- and ATR-induced primary ciliogenesis promotes cisplatin resistance in pancreatic ductal adenocarcinoma. J Cell Physiol 237: 4487-4503, 2022.
12. Wei L, Ma W, Cai H, Peng SP, Tian HB, Wang JF, Gao L and He JP: Inhibition of ciliogenesis enhances the cellular sensitivity to temozolomide and ionizing radiation in human glioblastoma cells. Biomed Environ Sci 35: 419-436, 2022.
13. Ma W, Wei L, Jin L, Ma Q, Zhang T, Zhao Y, Hua J, Zhang Y, Wei W, Ding N, *et al*: YAP/Aurora A-mediated ciliogenesis regulates ionizing radiation-induced senescence via Hedgehog pathway in tumor cells. Biochim Biophys Acta Mol Basis Dis 1870: 167062, 2024.
14. Jenks AD, Vyse S, Wong JP, Kostaras E, Keller D, Burgoyne T, Shoemark A, Tsalikis A, de la Roche M, Michaelis M, *et al*: Primary cilia mediate diverse kinase inhibitor resistance mechanisms in cancer. Cell Rep 23: 3042-3055, 2018.
15. Lee C, Yi J, Park J, Ahn B, Won YW, Jeon J, Lee BJ, Cho WJ and Park JW: Hedgehog signalling is involved in acquired resistance to KRA^{SG12C} inhibitors in lung cancer cells. Cell Death Dis 15: 56, 2024.
16. Khan NA, Willemarck N, Talebi A, Marchand A, Binda MM, Dehairs J, Rueda-Rincon N, Daniels VW, Bagadi M, Thimiri Govinda Raj DB, *et al*: Identification of drugs that restore primary cilium expression in cancer cells. Oncotarget 7: 9975-9992, 2016.
17. Guo R, Liu T, Shasaltaneh MD, Wang X, Imani S and Wen Q: Targeting adenylate cyclase family: New concept of targeted cancer therapy. Front Oncol 12: 829212, 2022.
18. Johnson JLF and Leroux MR: cAMP and cGMP signaling: Sensory systems with prokaryotic roots adopted by eukaryotic cilia. Trends Cell Biol 20: 435-444, 2010.
19. Brewer KK, Brewer KM, Terry TT, Caspary T, Vaisse C and Berbari NF: Postnatal dynamic ciliary ARL13B and ADCY3 localization in the mouse brain. Cells 13: 259, 2024.
20. Ou Y, Ruan Y, Cheng M, Moser JJ, Rattner JB and van der Hoorn FA: Adenylate cyclase regulates elongation of mammalian primary cilia. Exp Cell Res 315: 2802-2817, 2009.
21. Hong SH, Goh SH, Lee SJ, Hwang JA, Lee J, Choi IJ, Seo H, Park JH, Suzuki H, Yamamoto E, *et al*: Upregulation of adenylate cyclase 3 (ADCY3) increases the tumorigenic potential of cells by activating the CREB pathway. Oncotarget 4: 1791-1803, 2013.
22. Quinn SN, Graves SH, Dains-McGahee C, Friedman EM, Hassan H, Witkowski P and Sabbatini ME: Adenylyl cyclase 3/adenylyl cyclase-associated protein 1 (CAP1) complex mediates the anti-migratory effect of forskolin in pancreatic cancer cells. Mol Carcinog 56: 1344-1360, 2017.
23. Hu L, Dong C, Wang Z, He S, Yang Y, Zi M, Li H, Zhang Y, Chen C, Zheng R, *et al*: A rationally designed fluorescence probe achieves highly specific and long-term detection of senescence in vitro and in vivo. Aging Cell 22: e13896, 2023.
24. Yang Y, Li S, Wang Y, Zhao Y and Li Q: Protein tyrosine kinase inhibitor resistance in malignant tumors: Molecular mechanisms and future perspective. Signal Transduct Target Ther 7: 329, 2022.
25. Kim SO, Kim BY and Lee KH: Synergistic effect of anticancer drug resistance and Wnt3a on primary ciliogenesis in A549 cell-derived anticancer drug-resistant subcell lines. Biochem Biophys Res Commun 635: 1-11, 2022.
26. Duffy MP, Sup ME and Guo XE: Adenylyl cyclase 3 regulates osteocyte mechanotransduction and primary cilium. Biochem Biophys Res Commun 573: 145-150, 2021.
27. Sterpka A and Chen X: Neuronal and astrocytic primary cilia in the mature brain. Pharmacol Res 137: 114-121, 2018.
28. Hilgendorf KI, Myers BR and Reiter JF: Emerging mechanistic understanding of cilia function in cellular signalling. Nat Rev Mol Cell Biol 25: 555-573, 2024.
29. Kiseleva AA, Korobeynikov VA, Nikonova AS, Zhang P, Makhov P, Deneka AY, Einarson MB, Serebriiskii IG, Liu H, Peterson JR and Golemis EA: Unexpected activities in regulating ciliation contribute to off-target effects of targeted drugs. Clin Cancer Res 25: 4179-4193, 2019.
30. Guen VJ and Prigent C: Targeting Primary ciliogenesis with small-molecule inhibitors. Cell Chem Biol 27: 1224-1228, 2020.
31. Collinson R and Tanos B: Primary cilia and cancer: A tale of many faces. Oncogene 44: 1551-1566, 2025.

32. Saito M, Otsu W, Miyadera K and Nishimura Y: Recent advances in the understanding of cilia mechanisms and their applications as therapeutic targets. Front Mol Biosci 10: 1232188, 2023.
33. Pant K, Richard S, Peixoto E, Baral S, Yang R, Ren Y, Masyuk TV, LaRusso NF and Gradilone SA: Cholangiocyte ciliary defects induce sustained epidermal growth factor receptor signaling. Hepatology 81: 1132-1145, 2025.
34. Yin F, Chen Q, Shi Y, Xu H, Huang J, Qing M, Zhong L, Li J, Xie L and Zeng X: Activation of EGFR-Aurora A induces loss of primary cilia in oral squamous cell carcinoma. Oral Dis 28: 621-630, 2022.
35. Kasahara K, Aoki H, Kiyono T, Wang S, Kagiwada H, Yuge M, Tanaka T, Nishimura Y, Mizoguchi A, Goshima N and Inagaki M: EGF receptor kinase suppresses ciliogenesis through activation of USP8 deubiquitinase. Nat Commun 9: 758, 2018.
36. Tsai YC, Kuo TN, Chao YY, Lee PR, Lin RC, Xiao XY, Huang BM and Wang CY: PDGF-AA activates AKT and ERK signaling for testicular interstitial Leydig cell growth via primary cilia. J Cell Biochem 124: 89-102, 2023.
37. Lee JE, Park HS, Lee D, Yoo G, Kim T, Jeon H, Yeo MK, Lee CS, Moon JY, Jung SS, *et al*: Hippo pathway effector YAP inhibition restores the sensitivity of EGFR-TKI in lung adenocarcinoma having primary or acquired EGFR-TKI resistance. Biochem Biophys Res Commun 474: 154-160, 2016.
38. Guo Y, Dupart M, Irondelle M, Peraldi P, Bost F and Mazure NM: YAP1 modulation of primary cilia-mediated ciliogenesis in 2D and 3D prostate cancer models. FEBS Lett 598: 3071-3086, 2024.
39. Lee J, Park KC, Sul HJ, Hong HJ, Kim KH, Kero J and Shong M: Loss of primary cilia promotes mitochondria-dependent apoptosis in thyroid cancer. Sci Rep 11: 4181, 2021.
40. Jeffries EP, Di Filippo M and Galbiati F: Failure to reabsorb the primary cilium induces cellular senescence. FASEB J 33: 4866-4882, 2019.
41. Ma X, Zhang Y, Zhang Y, Zhang X, Huang Y, He K, Chen C, Hao J, Zhao D, LeBrasseur NK, *et al*: A stress-induced cilium-to-PML-NB route drives senescence initiation. Nat Commun 14: 1840, 2023.
42. Breslin L, Prosser SL, Cuffe S and Morrison CG: Ciliary abnormalities in senescent human fibroblasts impair proliferative capacity. Cell Cycle 13: 2773-2779, 2014.
43. Teng YN, Chang HC, Chao YY, Cheng HL, Lien WC and Wang CY: Etoposide triggers cellular senescence by inducing multiple centrosomes and primary cilia in adrenocortical tumor cells. Cells 10: 1466, 2021.
44. Liu X, Wei L, Zhang R, Chen J, Zhang T, Hua J, Wang J, He J and Xie X: The DNA-PKcs-primary cilia axis maintains ionizing radiation-induced senescence in tumor cells. Acta Biochim Biophys Sin, 2025. Doi: 10.3724/abbs.2025168.
45. Zhang H, Liu Y, Liu J, Chen J, Wang J, Hua H and Jiang Y: cAMP-PKA/EPAC signaling and cancer: The interplay in tumor microenvironment. J Hematol Oncol 17: 5, 2024.
46. Ginsberg G, Angle K, Guyton K and Sonawane B: Polymorphism in the DNA repair enzyme XRCC1: Utility of current database and implications for human health risk assessment. Mutat Res 727: 1-15, 2011.
47. Zou T, Liu J, She L, Chen J, Zhu T, Yin J, Li X, Li X, Zhou H and Liu Z: A perspective profile of ADCY1 in cAMP signaling with drug-resistance in lung cancer. J Cancer 10: 6848-6857, 2019.